

Airglow observation over equatorial and low-latitudes in the extreme solar minimum of 2007-2008

P K Rajesh^{1,§,*}, J Y Liu¹, C H Lin², A B Chen³, R R Hsu³ & H T Su³

¹Institute of Space Science, National Central University, Chung-Li, Taiwan

²Earth Dynamic System Research Center, National Cheng Kung University, Tainan, Taiwan

³Department of Physics, National Cheng Kung University, Tainan, Taiwan

[§]E-mail: pkrajesh@jupiter.ss.ncu.edu.tw

Received October 2011; accepted 23 February 2012

This paper reports the airglow observations in the extreme solar minimum period of 2007-2008 over low-latitude and equatorial regions. The observations are carried out using Imager of Sprites and Upper Atmospheric Lightning (ISUAL), onboard FORMOSAT-2 satellite. The ISUAL takes limb images of the emissions centered at 630.0 nm, viewing towards the right when the satellite is in the ascending orbit. The images are analysed to investigate the airglow intensity in the solar minimum years and also the latitudinal enhancement peaks in the emission. The results indicate that in the quiet conditions during 2007-2008, the seasonal variations are less pronounced.

Keywords: Airglow intensity, Thermosphere, Ionospheric irregularities, Solar flux, Limb imaging

PACS Nos: 94.20.Ac; 94.20.dt; 96.60.qd

1 Introduction

Thermosphere and ionosphere are usually influenced by several processes such as variations in solar irradiance, solar wind and magnetosphere input during active and disturbed conditions, energy transfer from lower atmosphere in terms of gravity waves, tides etc¹⁻³. Many such factors result in drastic fluctuations in plasma density by seeding or favouring instability processes that cause ionospheric irregularities over equatorial and low-latitude region⁴. The associated variations in electron density could influence satellite communications and hence, have drawn a great deal of attention of the scientific community. Such phenomena tend to occur more frequently during active solar phases, and much of the ionospheric observations and analysis pertain to high solar activity periods. This has resulted in some sort of bias in our understanding of background ionospheric behaviour and variations in the absence of external forcing due to solar activity.

In this context, the just concluded solar cycle 23 is of significance because of the unusually prolonged low active period, with deep minimum conditions prevailing during 2006-2009. Especially in 2008, the Sun was extremely quiet with almost no sunspots or solar flares. There was no significant magnetic activity in this period, and the mean F10.7 index was

about 70. Such conditions ensure that measurements carried out in this period could give valuable information regarding various inherent processes and interactions within the ionosphere and thus, enable to understand and model the associated parameters and its variation, which could be representative of the background quiet ionosphere. In the present work, the ionospheric characteristics over equatorial and low-latitude region in the solar minimum period 2007-2008, are investigated using space-borne airglow observations by Imager of Sprites and Upper Atmospheric Lightings (ISUAL) onboard Taiwan Formosa satellite, FORMOSAT-2. ISUAL takes limb images at 630.0 nm emission in the ascending orbit, giving horizontal and vertical airglow intensity around the local mid-night sector. The high resolution images, with considerable overlap of successive scans ensure high quality measurements, revealing latitudinal and altitudinal enhancement features⁵.

2 FORMOSAT-2/ISUAL

FORMOSAT-2, from its sun-synchronous, circular, polar orbit (inclination 98.99°) at an altitude of about 891 km, makes 14 revolutions around the earth per day. ISUAL consists of a set of optical payloads onboard the satellite, including an intensified charge coupled device (CCD) imager,

a 6-channel spectrophotometer, and a dual-band array photometer⁶. Though primarily designed for the studies of transient luminous events (TLE) induced by thunderstorm activities, ISUAL also takes limb images of the upper atmosphere in different airglow wavelengths when the FORMOSAT-2 is in the ascending orbit in the night hemisphere. Currently it might be the only space-borne instrument taking the limb images of the upper atmosphere in the visible band. In this work, the 630.0 nm CCD images taken during 2007-2008 are used.

The imager has a horizontal field-of-view (FOV) of 20° and a vertical FOV of 5°, with a corresponding pixel dimension of 516×128. The spatial resolution is about 2.14 km pixel⁻¹ at the tangent location. Depending on the satellite pitch angle, ISUAL could image tangent altitudes between 30 and 330 km, while providing a significant latitudinal coverage. The wide bandwidth of 7 nm allows the two major airglow regions to be imaged by the ISUAL. One is the 630.0 nm emission from the thermospheric region resulting from the transition of atomic oxygen from the excited O(¹D) state to the ground state. The other emission is the hydroxyl [OH (9-3)] transitions from the mesospheric region. The present study mainly describes the O(¹D) 630.0 nm intensity variations during the observation period.

3 Observations and Results

In its ascending orbit, FORMOSAT-2 makes overhead passes around 2200 hrs LT, and ISUAL takes limb scans looking at right angles to the satellite track towards eastern longitudes. Figure 1 illustrates the viewing geometry for a particular track named R09. Usually, there are such 14 tracks, from R01 to R14, covering different longitudes. Tangent plane of the ISUAL limb scans lie in the local midnight sector. The ground projection of the line-of-sights in the figure indicates the volume of the emissions integrated to record the images. Vertical pixels in each frame measure the altitude distribution of the intensity. A sampling rate of approximately 30 sec ensures significant overlap of successive frames, producing high horizontal resolution and better quality images. Multiple limb scans taken over a given track can be merged together to create altitude-latitude maps of the emission, revealing various features that modify its intensity.

Figure 2 displays a selected set of such maps taken in 2007 and 2008, respectively in each column, when

the satellite was orbiting in the track R09. For this particular track, the tangent plane lies over the longitude of Taiwan. Each row in Fig. 2 corresponds to the observations made in different seasons. The first image in the left column is made by combining the individual scans taken for the observing geometry in Fig. 1. Each image reveals two different airglow layers corresponding to the O(¹D) and OH(9-3) emissions. The O(¹D) layer appears in patches, and often shows regions of very strong enhancements. Whereas the OH(9-3) layer is continuous over the entire latitude range plotted, and enhancements are mainly caused when the corresponding line-of-sights pass through regions of intense O(¹D) emission⁵. The following analysis and explanation are based on the O(¹D) layer within ±25° latitudes.

The first row shows the images taken in March, the equinox period, and in both the years the features are very similar, revealing very intense O(¹D) emission near the magnetic equator. A much weaker O(¹D) layer can also be seen at other latitudes in 2008. There is no strong enhancement in June, and the layer is seen over almost all the latitudes. Again, the characteristics in both the years are mostly identical. The features in September equinox are more-or-less

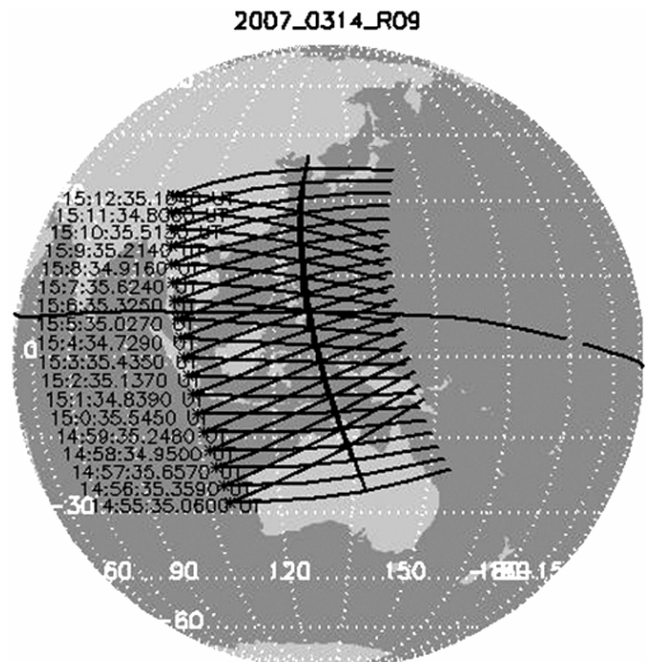


Fig. 1 — ISUAL trajectory and ground projection of the FOV (asterisk denotes the satellite track and thick curve parallel to the track is the tangent location, dark curve across the latitudes is the magnetic equator)

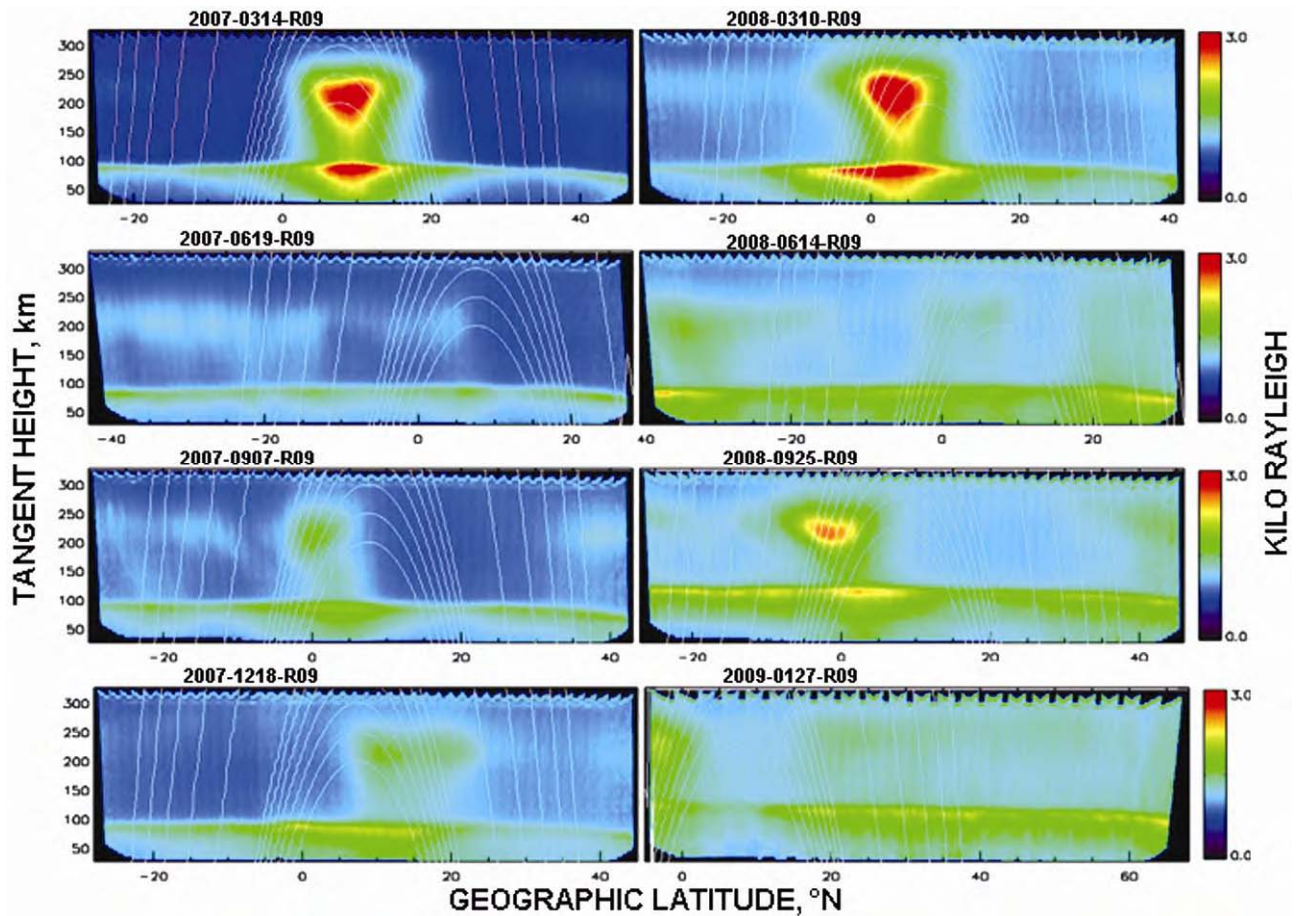


Fig. 2 — A set of selected examples of ISUAL images in 2007 (left), and 2008 (right) (top to bottom, the images represent March, June, September and December, respectively)

similar to that in the March equinox, showing mainly a single enhancement peak. An intense patch of $O(^1D)$ emission is seen between 5 and 25°N in December 2007. There is no $O(^1D)$ image in December 2008, and in the first available observation in January 2009 for this track, no such enhancement over the latitude region is seen. Unfortunately, there is no coverage over southern latitudes in this case, though an enhancement appears to exist just to the south of geographic equator.

Figure 3 gives the latitudinal profiles of the $O(^1D)$ intensity in different seasons in all the ISUAL observations in 2007. In the March equinox period, a pronounced equatorial enhancement can be seen with more or less uniform distribution of intensity in both the hemispheres. Similar enhancement near the equator is seen in the September equinox period also. The number of scans is very less in this case and the coverage in the southern hemisphere is less compared to that in the North. The peaks (location of maximum

intensity) in the emission appear closer to the magnetic equator ($\pm 10^\circ$) in the equinox months. In northern summer months, the distribution of the peaks indicates frequent occurrence in the northern hemisphere. In northern winter months, the observations are again less and also the coverage in the southern latitudes is limited. In summer and winter, the distribution of the peaks is wider ($\pm 20^\circ$). It is noted that the latitudinal profiles form two separate intensity groups in the March equinox and northern summer months. Such difference might be because the profiles from different longitude sectors are combined together in the figure. The simulations show a single peak in all seasons, which agree with the observed peaks in equinox months. In solstices, the peak is in the winter hemisphere, which agrees with the background meridional circulation and related ionospheric height variations.

Such limb images taken during 2007-2008 are used to understand how the airglow intensity behaves in

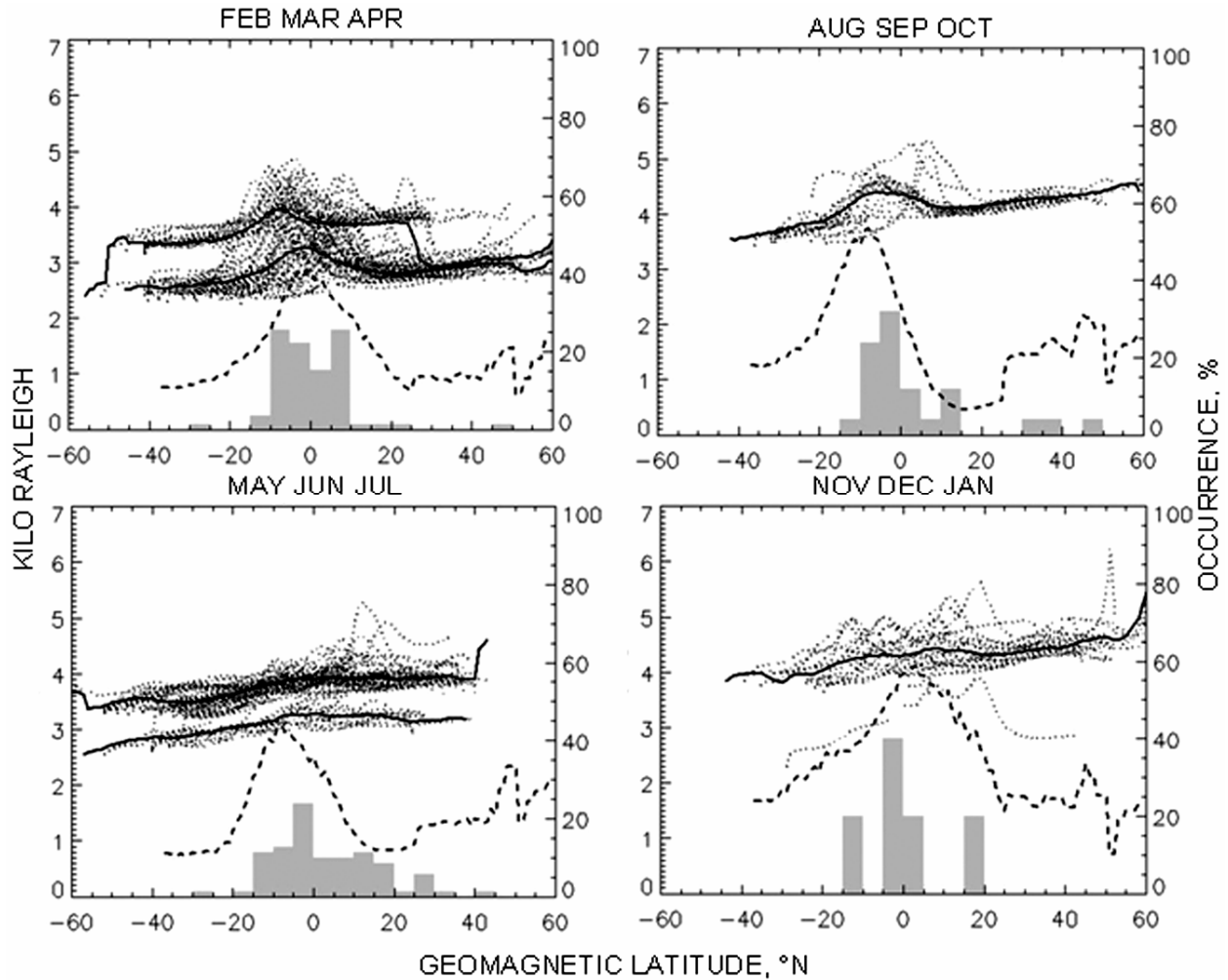


Fig. 3 — Latitudinal distribution of $O(^1D)$ intensity in different seasons in 2007 [dotted curve: individual scans in each season; solid dark lines: median values of these profiles; for the seasons when the individual profiles form distinct intensity levels, the median values are found for each such groups; histogram shows latitudinal distribution of the emission peaks (intensity maxima) in the $O(^1D)$ layer; dashed line gives the median latitudinal profile calculated by simulating the emission for each of the ISUAL tracks for every month]

this period. Figure 4 gives the average intensity over $20^\circ N$ latitude on each day in the years 2007 and 2008, after removing the background variation. The F10.7 solar flux index, used to denote the solar activity, shows a slight decline in its magnitude from the beginning of 2007 till end of 2008. There is a similar fall in the mean airglow intensity, though it is at much smaller level. Moreover, the intensity is more in the equinox period and shows lesser values in summer and winter months. This seasonal behaviour is least distinguishable in 2008. In addition to the observation, the 630.0 nm intensity during 2007-2008 is simulated using International Reference Ionosphere (IRI)⁷ and Mass Spectrometer Incoherent Scatter Radar⁸ models. The $O(^1D)$ volume emission is given by:

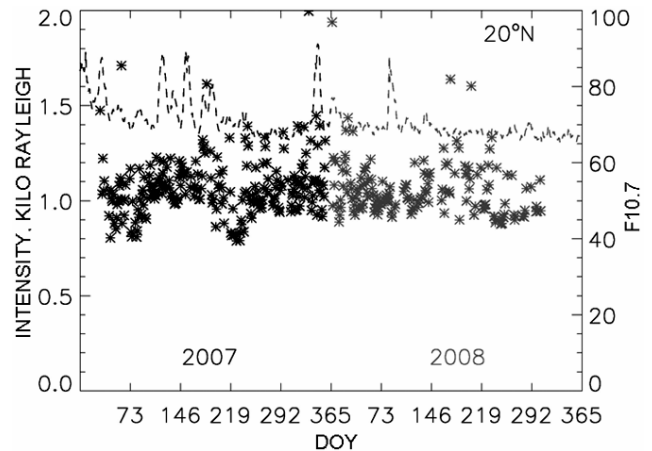


Fig. 4 — Average $O(^1D)$ intensity over $20 \pm 2^\circ N$ latitude from the entire observations in 2007 (dark shade) and 2008 (gray shade); dashed curve denotes the F10.7 index during the same period

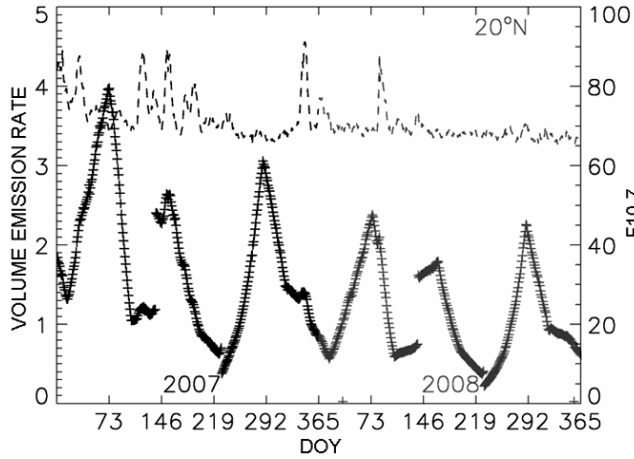


Fig. 5 — Simulated $O(^1D)$ volume emission rate over $20^\circ N$ latitude, at $121^\circ E$ longitude, in 2007 (dark shade) and 2008 (gray shade); dashed curve denotes the F10.7 index during the same period

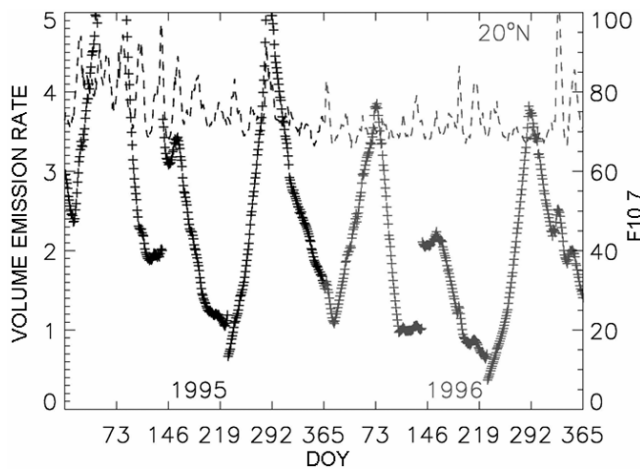


Fig. 6 — Simulated $O(^1D)$ volume emission rate over $20^\circ N$ latitude in 1995 (dark shade) and 1996 (gray shade); dashed curve denotes the F10.7 index during the same period

$$V_{630.0} = \frac{A_{1D} \mu_D \gamma_1 [O_2] [e]}{k_1 [N_2] + k_2 [O_2] + k_3 [O] + A_{1D} + A_{2D}}$$

where, A_{1D} , is the transition probability of 630.0 nm emission; and A_{2D} , that for the 636.4 nm emission; μ_D , the quantum yield of production of $O(^1D)$ state; γ_1 , the rate of the charge exchange process between O_2 and O^+ , producing O_2^+ ion; and k_1 , k_2 , and k_3 are the coefficients of collisional quenching of $O(^1D)$ state with N_2 , O_2 , and O , respectively²⁰. The intensity is simulated over $121^\circ E$ longitude and $20^\circ N$ latitude, and the result is plotted in Fig. 5. The simulation shows much rapid decrease in the intensity from the beginning of 2007 till the end of 2008. Further, the

seasonal variation is much more pronounced with distinct peaks in equinox, spring and autumn seasons. Similar simulation is carried out for the previous solar minimum period of 1995-1996 and the result is displayed in Fig. 6. The overall intensity in this period is slightly more than that in 2007-2008, but the variation is very similar in both the cases.

4 Discussion and Conclusion

The ISUAL observations in 2007 and 2008 in the corresponding months show overall similar characteristics. The strong enhancement over the equator (Fig. 2) have been reproduced in the simulations conducted earlier, when the input IRI electron density used had a broad single peak over the equator, especially near the tangent location⁵. The plasma density over equatorial region in the midnight period, travelling ionospheric disturbances, energetic particle precipitation, etc. could contribute to the observed latitudinal enhancements in the $O(^1D)$ intensity by modifying the photochemistry. The intensity of the 630.0 nm emission, which is produced by the dissociative recombination process is proportional to the plasma density⁹ and also is sensitive to F-layer height variations¹⁰⁻¹². The trans-equatorial neutral wind effect on the $O(^1D)$ emission is evident from the slightly stronger layer intensity in the winter hemisphere for the images taken in the months of June and December (Fig. 2).

In the equinox period, the inter-tropical arcs are usually located on both sides of the magnetic equator, while at solstice they appear in the winter hemisphere¹³. It can be seen from the latitudinal distribution of ISAUL $O(^1D)$ intensity that during the equinox months, the emission, in general, agree with this with most of the enhancement peaks above the equator. It is noted that the ISAUL observations are made at local midnight when the arcs are weak and most of the emission at this time is over the equator⁵. The electron density in March equinox, at 220 km, from Global Position System Occultation Experiment (GOX) onboard FOMOSAT-3/COSMIC satellites over the equator is about 2.05×10^5 electrons cm^{-3} , while it is about 3.05×10^4 electrons cm^{-3} and 7.32×10^4 electrons cm^{-3} , respectively at $20^\circ N$ and $20^\circ S$ latitudes at 2200 hrs LT, which agree with the observed intensity.

However, there are differences in some cases, with some of the scans showing peaks in the southern hemisphere in September equinox months and more

peaks appearing in the summer hemisphere in the solstice months. It can be speculated that such a difference could occur in case of an abatement or reversal of meridional wind, which are often associated with midnight temperature maximum (MTM)^{14,15}. Also, the O(¹D) intensity increases when the F-layer moves to lower altitudes where dissociative recombination occur faster. The post-midnight F-layer descent apparently occurs more frequently in summer hemisphere than in the winter hemisphere¹⁰. Further, the enhancement seen in the equinox over the equator could come from the more background density in this season. The peak electron density from GOX over the equator in March and September months are about 6.2×10^5 and 3.9×10^5 electrons cm^{-3} , respectively, while in June and December, the values are about 2.9×10^5 and 3.2×10^5 electrons cm^{-3} . The average peak altitude of the F-layer at the equator in March, June, September, and December are 290, 250, 320, and 305 km, respectively. In the solstice, the layer is more visible at most of the latitudes because of lower F-layer altitude.

The seasonal variation of the 630.0 nm intensity in the ISUAL measurement is consistent with that has been reported using photometer measurements over 20°N from India during the previous solar minimum period of 1994-1995 with peaks in the equinox months and smaller values in the winter period¹⁶. There are no ground based observations in the summer months over this region. The detailed seasonal and solar cycle variation of the 630.0 nm intensity at a similar latitude in the southern hemisphere over American longitude, during the low solar active years of 1975-1976, also confirms a similar seasonal tendency with peaks in the equinox period and lesser values in summer and winter months¹⁷.

The ISUAL observations indicate that the seasonal behaviour is less distinguishable during 2007-2008 compared to the measurements in the past solar minimum years^{16,17}. It may be noted that there could be longitudinal differences in the seasonal behaviour, and also in the previous report over the northern hemisphere, the seasonal coverage is limited¹⁶. Moreover, the limb observations by ISUAL are integrated over a range of longitudes, and hence the variations could also be suppressed. However, the simulations also suggest that the amplitude of the variation in the 2007-2008 is indeed smaller than the corresponding seasonal fluctuation in the 1995-1996

period. Ion temperature and O⁺/H⁺ transition height measurements in 2008 have indicated more cooling and contraction of the thermosphere than the expected levels in the prolonged periods of extremely low solar irradiance¹⁸. Further, thermospheric density records anomalously low values compared to the previous solar cycles¹⁹. The decrease in the density and temperature could play a role in the observed low fluctuations of the airglow intensity compared to the measurements in the past solar minimum periods.

In conclusion, the latitudinal distribution of the enhancement peaks in the O(¹D) intensity reveal more occurrence over the equatorial region in the equinox months and in the summer hemisphere in the June and December solstice period. The airglow intensity in the extreme solar minimum years of 2007-2008 seems to vary according to the solar flux and indicate that the seasonal fluctuations are less pronounced in this period.

Acknowledgements

The authors gratefully acknowledge the support by National Science Council Grants NSC98-2111-M-008-008-MY3 and NSC98-2116-M-008-006-MY3, to National Central University, Taiwan for the study.

References

- 1 Jacchia L J, Influence of solar activity on the earth's upper atmosphere, *Planet Space Sci (UK)*, 12 (1964) pp 355-378.
- 2 Rishbeth H, Long term changes in the ionosphere, *Adv Space Res (UK)*, 20 (1997) pp 2149-2155.
- 3 Lastovicka J, Forcing of the ionosphere by waves from below, *J Atmos Sol-Terr Phys (UK)*, 68 (2006) pp 479-497.
- 4 Kelley M C, *The Earth's ionosphere: plasma physics and electrodynamics* (Academic Press, New York), 1989.
- 5 Rajesh P K, Liu J Y, Chiang C Y, Chen A B, Chen W S, Su H T, Hsu R R, Lin C H, Hsu M-L, Yee J H & Nee J B, First results of the limb imaging of 630.0 nm airglow using FORMOSAT-2/Imager of sprites and upper atmospheric lightnings, *J Geophys Res (USA)*, 114 (2009) A10302, doi: 10.1029/2009JA014087.
- 6 Chern J L, Hsu R R, Su H T, Mende S B, Fukunishi H, Takahashi Y & Lee L C, Global survey of upper atmospheric transient luminous events on the ROCSAT-2 satellite, *J Atmos Sol-Terr Phys (UK)*, 65 (2003) pp 647-659.
- 7 Bilitza D, International Reference Ionosphere 2000, *Radio Sci (USA)*, 36 (2001) pp 261-275.
- 8 Hedin A E, Extension of the MSIS thermosphere model into the middle and lower atmosphere, *J Geophys Res (USA)*, 96 (1991) pp 1159-1172.
- 9 Peterson V L, Van Zandt T E & Norton R B, F-region nightglow emissions of atomic oxygen, 1: Theory, *J Geophys Res (USA)*, 71 (1996) pp 2255-2265.
- 10 Nelson G J & Cogger L L, Dynamical behavior of the nighttime ionosphere at Arecibo, *J Atmos Terr Phys (UK)*, 33 (1971) pp 1711-1726.

- 11 Bittencourt J A & Sahai Y, Behavior of the [OI] 6300 Å emission at the magnetic equator and its reaction to the vertical ExB drift velocity, *J Atmos Terr Phys (UK)*, 41 (1979) pp 1233-1239.
- 12 Herrero F A & Meriwether J W, 6300 Å airglow meridional intensity gradients, *J Geophys Res (USA)*, 85 (1980) pp 4194-4204.
- 13 Thuillier G, King J W & Slater A J, An explanation of the longitude variation of the O(¹D) 630 nm tropical nightglow intensity, *J Atmos Terr Phys (UK)*, 38 (1976) pp 155-158.
- 14 Colerico M, Mendillo M, Nottingham D, Baumgardner J, Meriwether J, Mirick J, Reinisch B W, Scali J L, Fesen C G & Biondi M A, Coordinated measurements of F-region dynamics related to the thermospheric midnight temperature maximum, *J Geophys Res (USA)*, 101 (1996) pp 26,783-26,793.
- 15 Burnside R G & Tepley C A, Airglow intensities observed in the southern and northern hemispheres, *Planet Space Sci (UK)*, 38 (1990) pp 1161-1177.
- 16 Mukerjee G K, Carlo L & Mahajan S H, 630 nm nightglow observations from 17° N latitude, *Earth, Planet Space (Japan)*, 52 (2000) pp 105-110.
- 17 Sahai Y, Takahashi H, Bittencourt J A, Sobral J H A & Teixeira N R, Solar cycle and seasonal variations of the low latitude OI 630 nm nightglow, *J Atmos Terr Phys (UK)*, 50 (1988) pp 135-140.
- 18 Heelis R A, Coley W R, Burrell A G, Hairston M R, Earle G D, Perdue M D, Power R A, Harmon L L, Holt B J & Lippincott C R, Behavior of the O⁺/H⁺ transition height during the extreme solar minimum of 2008, *Geophys Res Lett (USA)*, 36 (2009) L00C03, doi: 10.1029/2009GL038652.
- 19 Emmert J T, Lean J L & Picone J M, Record-low thermospheric density during the 2008 solar minimum, *Geophys Res Lett (USA)*, 37 (2010) L12102, doi: 10.1029/2010GL043671
- 20 Link R & Cogger L L, A re-examination of the OI 6300 Å nightglow, *J Geophys Res (USA)*, 93 (A9) (1988) pp 9883-9892.